BLUECOPTER DEMONSTRATOR: MASTERING DYNAMICS CHALLENGES

Raphael Rammer, Adrian Kus, Jean-Baptiste Maurice, Oliver Dieterich, Peter Konstanzer
Airbus Helicopters Deutschland GmbH, Donauwörth, Germany

Abstract

The BLUECOPTER DEMONSTRATOR was developed to prove the feasibility of future eco-friendly helicopters by demonstrating significant reduction of CO2 emission, fuel consumption and noise. The contributors to the improved efficiency and minimized acoustic emission are a newly developed main rotor system, an optimized Fenestron®, several drag reduction measures, a "T-Tail" horizontal stabilizer, an active fin rudder as well as an "acoustic liner" for the Fenestron® shroud. The demonstrator is based on the successful light/medium twin engine helicopter EC135 and has been successfully flight tested from 2014 to 2016.

This paper gives an overview of the challenges with respect to the helicopter dynamics resulting from the requirements for eco-friendliness. The innovative planform of the main rotor blades is treated as well as the low nominal tip speed and the large rotor speed range. The flexbeam was optimized to provide enhanced lead-lag damper kinematics for increased lead-lag damping compared to the EC135. The efforts to ensure flutter stability of the double swept planform are highlighted in the paper.

Modifications to the drive train were introduced. The tail rotor drive shaft had to be elongated and the tail gear box ratio had to be increased. Tests with a serial EC135 Fenestron® and an advanced BlueEdgeTM style Fenestron® were performed. Simulative studies on drive train torsion and bending dynamics were conducted prior to the BLUECOPTER DEMONSTRATOR test campaign and subsequently validated by ground and flight test results.

For achieving a permit to fly for the BLUECOPTER DEMONSTRATOR, ground and air resonance stability calculations were performed. To validate the models whirl tower, airframe shake test and lead-lag damper laboratory test results were used. A preliminary rotor speed envelope limitation was lifted after showing good agreement of the analysis with first test results.

NOMENCLATURE

AEO	All Engines Operative
C.G.	Center of Gravity
EC135	Twin engine helicopter, MTOW = 2.91 t
H145	Twin engine helicopter, MTOW = 3.70 t
MTOW	Maximum Take Off Weight
PWC	Pratt & Whitney Canada
OEI	One Engine Inoperative
$\Delta\Theta$	Change of blade pitch angle
$\Delta\zeta$	Change of blade lag angle
δ_1	Pitch-lag coupling angle
δ_3	Pitch-flap coupling angle

1. INTRODUCTION

Environmental protection is a key driver for modern aviation industry. Especially rotorcrafts suffer from external noise issues which deny operating rotorcrafts to a large extent in urban environment and thus do not allow fully exploiting the rotorcraft capabilities of VTOL in cities. Thus, increased attention is paid during rotorcraft design phases to the growing public concern about air pollution, noise and climate change.

The "BLUECOPTER DEMONSTRATOR" (Figure 1) has been developed to prove the feasibility of future eco-friendly helicopter concepts by demonstrating significant reduction of CO2 emission, fuel consumption and noise.

Figure 1: BLUECOPTER DEMONSTRATOR

The demonstrator is based on the successful

light/medium twin engine helicopter EC135 used as a test bed for a set of innovative technologies. In the meantime the EC135 was upgraded and renamed H135 [1]. However, the BLUECOPTER DEMONSTRATOR is based on the original version. Focus of the demonstrator design was put on reducing the power required by the aircraft, a smart power management and several measures to minimize the acoustic footprint.

A main contributor to the improved efficiency and minimized acoustic emission is the newly developed main rotor system with its innovative five bladed bearingless design. Other contributors are the optimized Fenestron®, several drag reduction measures at airframe and rotor including a “T-Tail” horizontal stabilizer.

Additional features like an active fin rudder and an “acoustic liner” for the Fenestron® shroud are applied to further improve the acoustic footprint of the demonstrator. The BLUECOPTER DEMONSTRATOR was successfully flight tested from 2014 to 2016. Information on the acoustics results can be found in [2].

Based on [3] this paper gives an overview of the challenges with respect to the helicopter dynamics resulting from the requirements for eco-friendliness starting with the main rotor as key component for the achieved improvements. The main rotor system combines the first time modern rotor technology in terms of the bearingless main rotor (BMR) concept with a BlueEdge^{TM} type blade planform in order to realize the acoustic benefits of such blades. The evolution of double-swept blades originated from the ERATO project - a joint DLR-ONERA research culminating in the manufacturing and extensive wind tunnel testing of a model rotor system of 2.1 m radius. Due to the technical success of the ERATO project, next step in the evolution consisted in the development of a full scale blade demonstrator by Airbus Helicopters and ONERA flown on the EC155 (Figure 2) and hereby fulfilling the high expectations [4].

Figure 2: BlueEdge^{TM} demonstrator on EC155

Therefore, it was a logical step to pour the BlueEdge^{TM} technology into serial products as now visible on the H160 (Figure 3). A detailed overview of BlueEdge^{TM} and the successful transfer from research into serial application is presented in a recent paper, see [5].

Due to its double swept blade planform, it is obvious that such kind of blades need special aeroelastic attention in view of significantly coupled blade modes. Offsets of mass and stiffness axes in the double-swept part of the blade lead to pronounced mixture of flap and torsion motions and loads – a feature especially to be monitored during the flutter studies of the main rotor system.

Figure 3: H160 featuring BlueEdge^{TM}

Nevertheless, the selection of the advanced blade planform is not the only means to reduce the acoustic footprint and to improve the performance. While the serial EC135 features a quite compact main rotor design in terms of diameter and solidity, the BLUECOPTER DEMONSTRATOR main rotor is significantly increased in diameter and chord in addition to a fifth main rotor blade. These characteristics allow the main rotor to be operated at lower tip speed compared to classical designs and serial applications. On the other hand, the increased weight of the main rotor and the increased sensitivity to unsteady air loads asks for dedicated analysis of ground and air resonance. Coupling phenomena such as ground and air resonance can be understood as feedback systems of the rotor coupled to the airframe. High rotor sensitivity to disturbances corresponds to high feedback gains known to have the potential to degrade stability of the entire vehicle. On the other hand the EC135 family is known to show adequate performance in these disciplines.

In addition to the low rotor speed, the range of rotor speed variation is significantly increased e.g. when comparing to the already large range of the H145 spanning from 96% to 107%. The related potential of optimization for acoustic and performance purposes needs to be enabled by an adequate frequency

placement of the dynamic system – not only in view of the dynamic layout of the main rotor system but also with respect to drive train dynamics in order to avoid critical frequency crossings and to ensure adequate frequency separation of natural frequencies from rotor or shaft speed.

Further peculiarities of the BLUECOPTER DEMONSTRATOR such as the T-tail, the active rudder and the advanced blades of the Fenestron® proved to be less challenging in view of dynamics. Due to the enlarged lever arm, the T-tail design allowed to reduce the size of the horizontal stabiliser significantly. In addition, the size of the vertical fin also benefits from the T-tail due to the end plate effect of the horizontal stabilizer on top of the vertical fin. These design features culminated in an easy fulfilment of tail flutter requirements although the flight speed range is close to EC135. The active rudder – although a quite unknown device for rotorcrafts – is somehow comparable to conventional rudders of the fixed wing world and does not pose significant design challenges. Concerning the BlueEdge™ style Fenestron® blades, no serious aeroelastic challenges are raised hereby as such kind of blades are quite stiff – also visible by the low Lock number being about one order less than for main rotor systems.

The development of the main rotor system as key component of the BLUECOPTER DEMONSTRATOR dates back to the German research projects ECO-HC, IKOROZ and LoCAR under the framework of Lufo IV. Focus was not only put on aeromechanics aspects [6], [7] but also on other disciplines such as materials and manufacturing [8], [9].

The flight test campaign of the BLUECOPTER DEMONSTRATOR was launched mid of 2014 and lasted until begin of 2016. No stability issues were reported during the entire flight test campaign although a large variety of configurations and operating conditions were tested hereby proving the selected approach for mastering the various dynamic challenges.

This paper details the main dynamic issues of the BLUECOPTER DEMONSTRATOR by highlighting in the following section dynamic characteristics of the main rotor system with its special characteristics of blade planform, low rotor speed and large speed variations. Afterwards, the next part is dedicated to the interference of the main rotor system with the drive train system and the required design modifications compared to the serial EC135. Section 4 closes with the coupling characteristics of the main rotor system with the airframe on ground and in flight in order to check impact of the increased size of the main rotor system on ground and air resonance stability.

2. ROTOR DYNAMICS

An innovative double swept planform was chosen for the blade's design mainly to meet noise reduction requirements during approach. This kind of blade planform branded by AIRBUS Helicopters as BlueEdge™ allows significantly reducing BVI (blade vortex interaction) noise by its double swept leading edge design avoiding parallelism with tip vortices. On the other hand, it favors coupling between flap and pitch motions.

For fuel efficiency and acoustics reasons a low nominal tip speed and a large rotor speed range were selected for the BLUECOPTER DEMONSTRATOR. The low tip speed required a large mean chord. The resulting blade mass eased the fulfillment of requirements for large blade inertia for sufficient autorotation behavior.

The innovative planform and large rotor speed range required special care during the dynamic layout phase of the blade.

2.1. Blade Tuning

Low vibratory hub loads were not a primary target for this rotor. However, an adequate blade frequency tuning with reasonable effort was aimed at. The large rotor speed range made this task an ambitious one as flap and lag are differently affected by centrifugal loading.

The blade layout was performed by means of the in-house rotor dynamics code MOSES (uncoupled calculation of beams in centrifugal field) and in later stages by CAMRAD II [10], Figure 4.

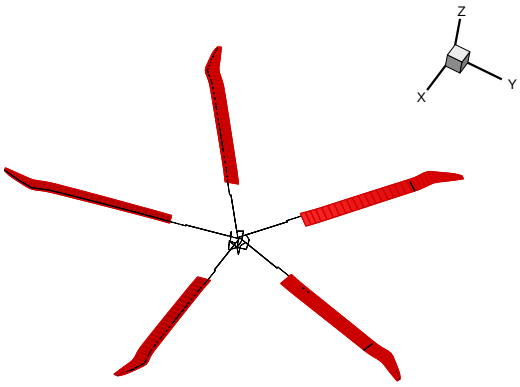

Figure 4: CAMRAD II model of BLUECOPTER DEMONSTRATOR main rotor

General dynamic design philosophy is to locate the rotor frequencies in a way to avoid resonances with rotor harmonics. However, due to the planform and large rotor speed range compromises had to be accepted.

To reduce the weight of tuning masses a flap frequency near the 3/rev frequency was agreed to. The resulting blade loads will not be transformed from rotating to fixed system, but increase dynamic loads of the blade. This was judged acceptable by fatigue analysis.

For the placement of the second lead-lag mode also a compromise was accepted. For parts of the rotor speed range it is close to the 6/rev frequency. This can lead to amplification of inplane hub forces, but the risk was taken to reduce tuning effort and mass penalties. It was assumed for a bearingless main rotor that the inplane forces are significantly lower than the hub bending moments resulting form 4/rev and 6/rev harmonics.

The frequency tuning also was influenced by limitations due to the blade planform. It was not possible to place tuning masses close to the blade tip, as it is swept backwards behind the control axis. A tuning mass in this range required compensation in an area where the blade is swept forward due to flutter stability. The forward swept area was not an ideal place for tuning higher flap and lead-lag bending modes.

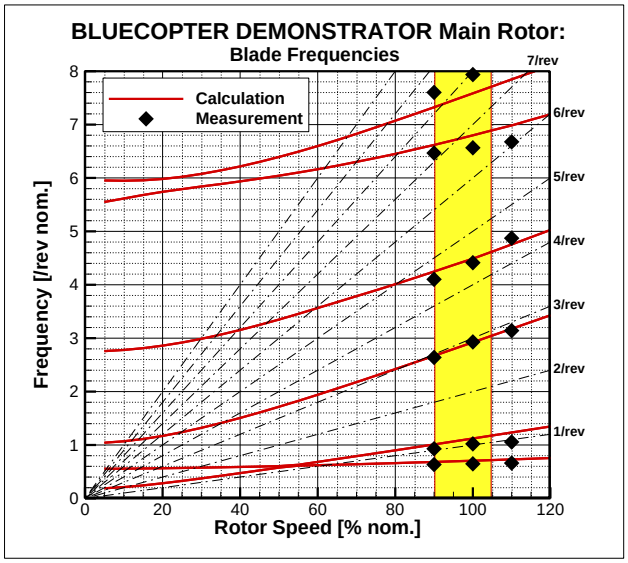

Figure 5: Fan diagram showing calculations and whirltower measurement

The outcome was a total amount of tuning mass of approximately 5 kg, including balancing provisions, mass for lock number reduction and masses for frequency placing, enabling an acceptable blade layout.

The main rotor was tested on the whirltower to verify calculation models and to achieve a permit to fly for the BLUECOPTER DEMONSTRATOR.

Figure 5 shows a fan diagram for the whirltower case with calculation results and whirltower measurements. The second flap mode frequency was met nearly exactly by the calculations, the third flap mode also fits adequately, which was a strong design goal due to the significant impact of this mode on the vibratory hubs loads.

Higher frequencies showed less agreement between calculation and test than the second and third flap mode. The reason for this is assumed to be found in the blade's planform, which favors coupling effects between modes. The placement of blade axes (elastic, tension, center of gravity) and the mass distribution has to be much more exact than for a straight blade.

The control configuration on the whirltower is known to be significantly stiffer than on the helicopter, leading to higher second lead-lag frequency values due to mode coupling phenomena with torsion than on the helicopter.

2.2. Couplings with Pitch Mode

Two coupling phenomena with the first pitch mode are of importance. The pitch-flap coupling (δ_3), which describes the pitch motion of the blade due to a flapping motion, is of interest for handling qualities of a helicopter. The pitch-lag coupling (δ_1), which describes the pitch motion of the blade due to a lagging motion is of importance for the lead-lag damping behavior of the blade versus collective angle setting.

Pitch-flap coupling: The pitch flap coupling angle was calculated for an elastic flexbeam, blade and mast combination. The mast flexibility was introduced by an attachment spring for the blade at the hub in the model. The spring was tuned according to whirltower and flight test results. The attachment stiffness of the BLUECOPTER DEMONSTRATOR's rotor hub is in a range where zero δ_3 coupling occurs.

Pitch-lag coupling: The BLUECOPTER DEMONSTRATOR's controls were designed to deliver increasing pitch flap coupling versus collective angle setting in contrast to EC135, which features a decreasing characteristic versus collective angle, see Figure 6. The lead-lag coupling angle δ_1 (arctan($\Delta\Theta/\Delta\zeta$)) is shown in the figure.

The BLUECOPTER DEMONSTRATOR's pitch horns are placed at the trailing edge, the EC135's pitch horns at the leading edge. The characteristics were calculated for an elastic flexbeam and blade accounting for uniform inflow aerodynamics.

The pitch-lag coupling characteristic of the BLUECOPTER DEMONSTRATOR's main rotor supports lead-lag damping during flight.

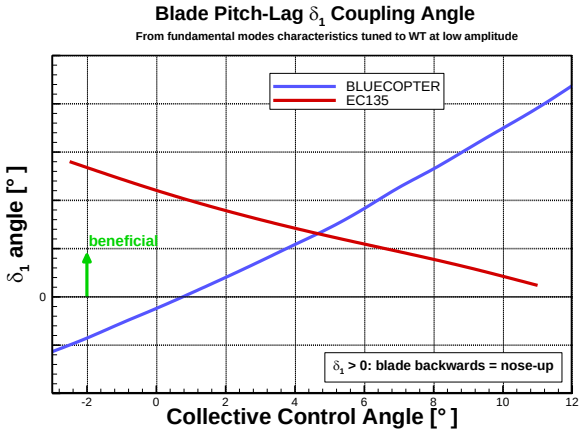

Figure 6: Pitch-lag coupling angle

2.3. Lead-Lag Damping

The latest version of the EC135 elastomeric lead-lag damper was used for the BLUECOPTER DEMONSTRATOR's main rotor blades. The flexbeam design was optimized to significantly increase the lead-lag damping of the new rotor by an enhanced lead-lag stiffness distribution, which ensured significantly better damper kinematics than for the EC135 main rotor blades. This was required in view of large blade inertia.

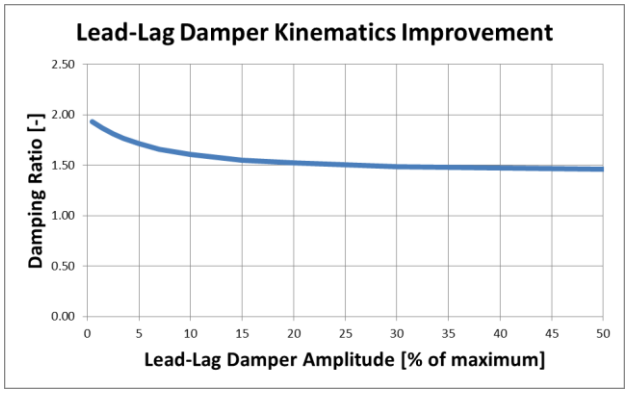

Figure 7: Improvement of lead-lag kinematics for BLUECOPTER DEMONSTRATOR rotor versus EC135 rotor

Figure 7 shows the ratio of lead-lag damping (the damping is related to a loss factor of 1 to compare the kinematics) between the BLUECOPTER DEMONSTRATOR rotor and the EC135 rotor. The improvement is in the range of a factor of 1.5. This results in lead-lag damping and frequency characteristics versus lead-lag angle, shown in Figure 8. Here, the damping characteristic for a maximum stiff damper, according to specification, at 25°C is shown. The stiffness dependency on the damper amplitude can clearly be seen in the figure.

As the lead-lag damper is the same than for the EC135, the modal damping increase compared to EC135 is approximately in the same range than shown in Figure 7 for the damper kinematics properties.

The lead-lag damping calculations, mentioned above, were performed with a model neglecting cone angle effects and mode coupling.

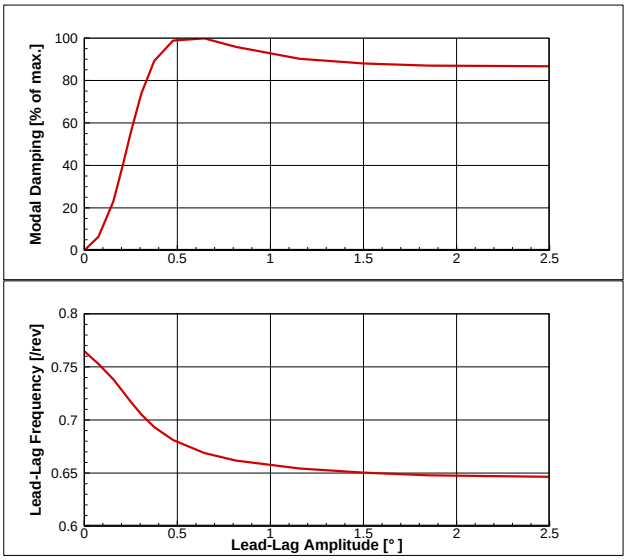

Figure 8: Modal damping and lead-lag frequency versus lead-lag amplitude

Prior to whirltower testing the characteristics of the first lead-lag mode were investigated by a more sophisticated model taking aerodynamics, mode coupling and control kinematics into account. This model was updated after component tests with the lead-lag dampers, flexbeams and blades and whirltower testing.

The lead-lag damper component tests were performed with all five damper pairs, actually integrated in the rotor, to investigate its non-linear behavior versus deflection amplitude, frequency and loading history.

The updated model was used to achieve the permit to fly for the BLUECOPTER DEMONSTRATOR. Figure 9 shows a comparison of lead-lag mode frequency and damping between calculation and whirltower test results. A good agreement between calculation and measurement can be seen. The whirltower data was used to achieve a proper setup for the calculation models in terms of lead-lag damper non-linearity and therewith improve ground and air resonance calculations.

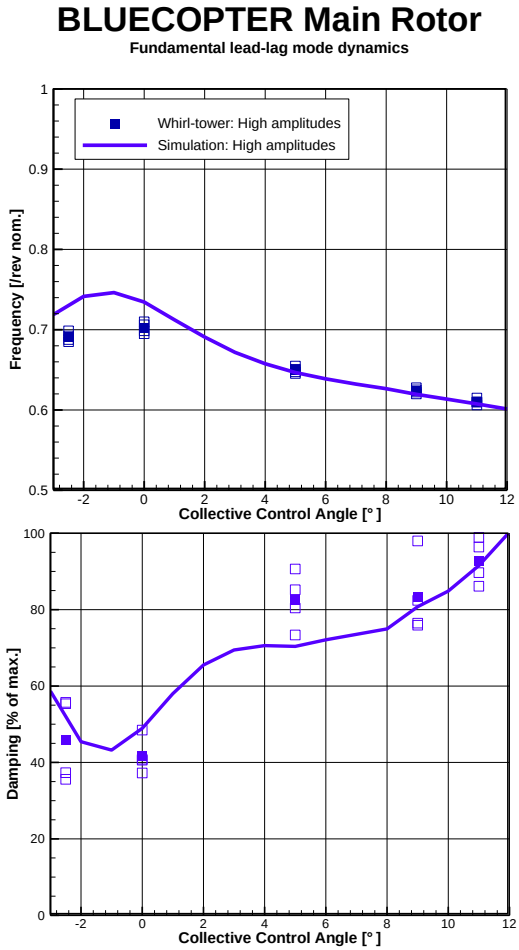

Figure 9: Comparison between calculation and whirltower testing

2.4. Flutter Stability

Significant effort was pursued in the blade design to ensure flutter stability of this challenging double swept blade plan form by means of aero-elastic multi-body calculations accounting for aerodynamics and control stiffness.

First a simple investigation on the chordwise position of the blade's center of gravity and its aerodynamic center was performed. It was shown that the center of gravity lies well in front of the aerodynamic center. Due to the placement of a large tuning mass at the most forward position this blade has a better chordwise C.G. position than some serial blades. This gave first confidence in the design.

Afterwards calculations were performed at rotor overspeed conditions (NR higher than maximum operative speed, for adding conservatism). Variations of blade C.G. and control stiffness were investigated as well as high speed flight conditions for different weight configurations.

Table 1: Parameter modifications, investigated regarding sensitivity on flutter stability

Parameter	Magnitude of modification
Main rotor speed	+ 10% (of max. operative NR)
Shift of chordwise C.G.	+ 10 % (mean blade chord)
Control stiffness	- 90% (one order of magnitude)

Table 1 lists the magnitude of modifications which were investigated in order to study the impact of offsets from the nominal design on flutter stability margins.

These values show that for the BLUECOPTER DEMONSTRATOR's main rotor, no flutter instability had to be expected.

On the whirltower, a test with significantly increased rotor speed was performed. This confirmed the robust blade design regarding flutter, in-line with high speed flight tests where no flutter tendency was present.

2.5. Whirltower Test / Validation

The rotor properties were verified on the whirl tower. Figure 10 shows a photograph of the BLUECOPTER DEMONSTRATOR's main rotor mounted on the test bench.

Figure 10: BLUECOPTER DEMONSTRATOR rotor on the whirltower

The predictions for lead-lag damping and the test results matched very well. A comparison was already presented in Figure 9. The demonstration of sufficient damping was important for the achievement of the permit to fly.

For aeroelastic stability verification the rotor was operated at 125% overspeed on the whirl tower. Figure 11 shows rotor speed, which was increased from 100% to 125%, pitch link force (red), flap

bending moment (purple) and torsion moments (turquois and green). No tendency of unstable behavior was detected.

A good agreement between calculations and testing can be shown for the most relevant blade frequencies. A fan diagram with calculation and measurement results already was shown in Figure 5.

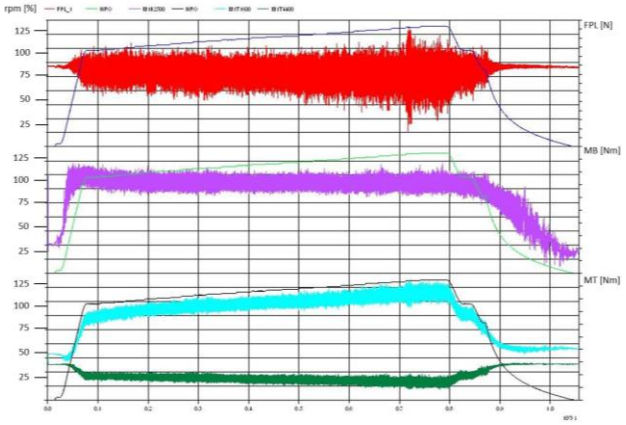

Figure 11: Rotor speed, pitch link force, flap bending moment and torsion moments for an overspeed test run

3. DRIVE TRAIN DYNAMICS

In order to provide a suitable drive train system for the BLUECOPTER DEMONSTRATOR test bed, an adaptation of the serial EC135 drivetrain was required for the demonstrator.

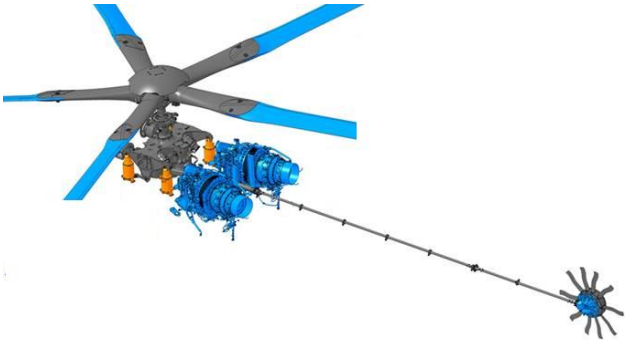

Figure 12: BLUECOPTER drive train architecture

The elongated tail boom was accounted for by modifying shaft segments of the EC135 tail drive shaft. It should be kept in mind that although most parts (including MGB) were reused, the drive train system was operated at reduced speed in order to account for the low main rotor speed. Solely the TGB ratio had to be increased in order to retain the Fenestron® rotor speed, thus allowing using the serial EC135 Fenestron® in a first step. In a second step, the rotor blades have been replaced by advanced BlueEdge™ style Fenestron® blades featuring an aero-acoustically optimized shape. Simulative studies on drive train torsion and bending dynamics have been performed prior to the BLUECOPTER DEMONSTRATOR test campaign and subsequently validated by ground and flight test results.

3.1. Drive Train Torsion Stability

The low main rotor tip speed, aiming at reduced noise emission, together with the target to use the EC135 serial drive train as a basis leads to a significantly reduced nominal drive train speed compared to the EC135. However, in combination with the high main rotor inertia, the BLUECOPTER drive train features a higher rotational energy than EC135. Considering that PWC engines similar to those of the EC135 are used, the main adaption regarding torsional stability focused on the engine control laws and the frequency placement of associated signal filters.

Prior to ground and flight testing, the stability of the closed-loop feedback system, consisting of the mechanical drive train coupled with the engine control system, has been assessed through a comprehensive simulation approach, based on the Airbus Helicopter's in-house toolbox GAHEL [11]. This has enabled to appropriately setup the engine control software, including frequency placement of signal filters according to drive train torsion eigenmodes.

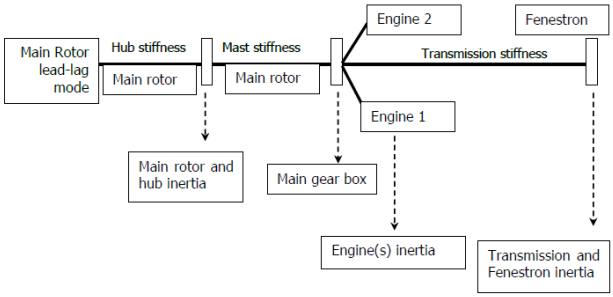

Figure 13: Drive train simulation model (6-DOF)

In close cooperation with the engine manufacturer Pratt & Whitney Canada, the simulation environment has been established in a two-step approach where Airbus Helicopters has put focus on the drive train modeling part while PWC has contributed engine control models. As schematically illustrated in Figure

13, a six degree of freedom drive train model has been created by Airbus Helicopters, representing stiffness and inertia data of the main drive train components (such as rotors, gear wheels, shafts, engines and accessories like generators or cooler fans) which are redistributed to a discrete number of rigid bodies while the main rotor lead-lag bending dynamics are considered additionally.
By coupling the drive train model with an engine model and the corresponding engine control feedback laws provided by PWC, closed-loop simulations have been performed for investigating the sensitivity of stability margins regarding the following parameters:

- Engine power turbine speed
  (linked to main rotor/drive train speed)
- Engine gas generator speed
  (represents different power conditions)
- Ambient conditions (altitude)
- AEO/OEI operating conditions
  (impacting drive train inertia and power settings)

Phase and gain margins of the closed-loop system have been identified based on the open loop transfer function (see Figure 14) for assessing stability. Thereby, as typical, AEO operation at high altitude has been identified as most critical, however still showing fully sufficient margins.

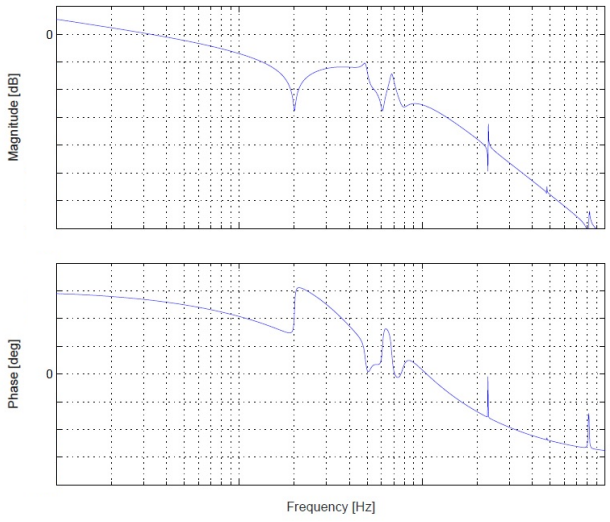

Figure 14: Transfer function of coupled engine - drive train model (NR commanded → NR)

Prior to first flight of the demonstrator, ground tests have been performed in order to confirm the simulation results and thus substantiate flight clearance regarding drive train torsion dynamics. Through step and sinusoidal (at varying frequency; see Figure 15) inputs on the collective M/R control, stable behavior has been demonstrated and eigenfrequencies of the drive train system have been identified. Similar step inputs have also been performed in flight for confirming ground test results at higher rotor loading and during forward flight conditions.

Ground test results have been used for validating the drive train simulation model and thus for complementing the simulation based design approach.

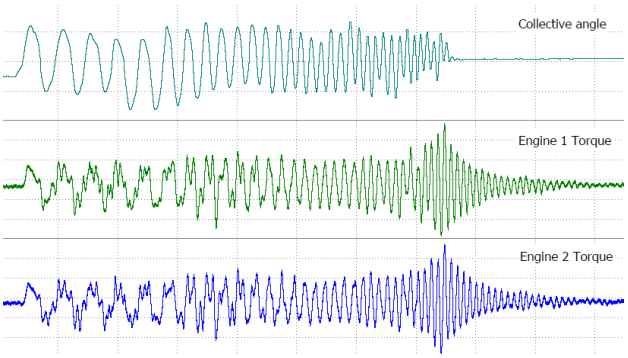

Figure 15: Excitation of drive train torsion oscillations (ground testing, AEO)

As shown in Figure 16, a very good match between measured and simulated eigenfrequency has been obtained showing a deviation of less than 4% for the non-adapted (initially set up) simulation model.

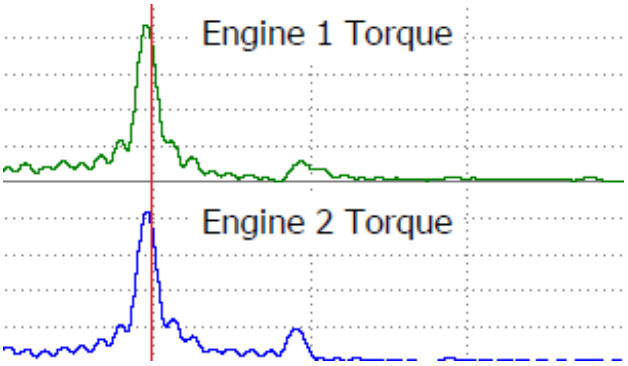

Figure 16: Measurement (frequency spectrum) vs. simulation result (vertical line) for the lowest frequent drive train torsion eigenmode (AEO)

Through the high accuracy of the simulation results, the capability of the simulation based approach (as applied for the BLUECOPTER DEMONSTRATOR and described here), has been demonstrated.

3.2. Critical Whirling Speeds

In order to avoid high loads due to dynamic amplification of excitations, for example coming from the main rotor unbalance or unbalances of the drive shafts, adequate frequency placement (i.e. with sufficient margins to excitation frequencies) of drive train torsion and bending eigenmodes is of major importance. Especially for the BLUECOPTER DEMONSTRATOR this imposed a significant challenge, as a drive train system close to the EC135 serial design was used while the nominal drive train speed was significantly reduced and the operative rotor speed range was considerably increased. These constraints substantially diminished the design corridor for the frequency placement. Besides considering critical torsion speeds, which focus on drive train torsion eigenfrequencies, bending dynamics of drive train components such as rotor mast whirl or shaft critical bending speeds were investigated. In the following, the dynamics layout of the tail rotor drive shaft with respect to critical bending will be highlighted.

The low main rotor speed in combination with a reuse of the EC135 serial Fenestron® leads to an increased amount of anti-torque required. Together with an increase of main rotor diameter this provoked an elongation of the tail boom which resulted in an adaption of the EC135 serial tail rotor drive shaft. Considering the design target to remain in subcritical operating condition, the elongation of the drive shaft required an additional bearing as well as stiffness adaption measures for single shaft segments in order to augment the bending eigenfrequencies.

Figure 17: Tail drive shaft simulation model for shaft bending modal analysis (FE model / NASTRAN)

During the design phase, a simulation model of the drive shaft was setup, in parallel using an in-house tool on the one hand and the commonly known Finite Element solver NASTRAN on the other hand (see Figure 17). As both tools feature different pros and cons, the tail rotor drive shaft design loop was used to verify that similar results are computed for the basic model setup. Besides investigating nominal operating conditions (including ground idle or in-flight autorotation conditions), failure cases for the shaft bearings were considered.

For confirming the predicted, adequate dynamic layout and validating the simulation model, a hammer impact test on the tail rotor drive shaft, mounted on the demonstrator, has been performed (see Figure 18). Due to the excellent accordance between simulation and test data (see Figure 19 for the frequency match) flight clearance regarding critical bending easily was granted.

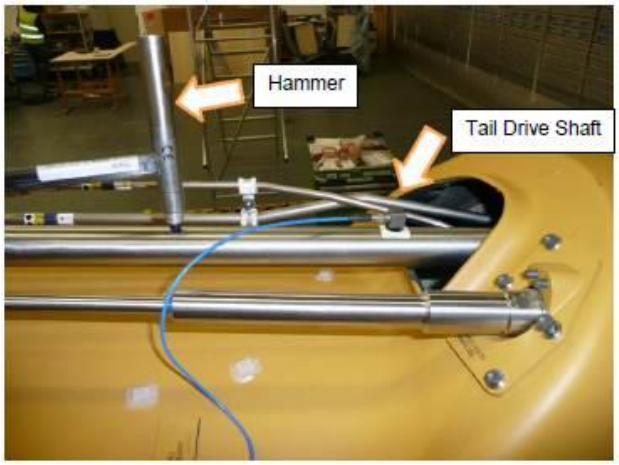

Figure 18: Modal testing (hammer impact test) on the BLUECOPTER tail rotor drive shaft

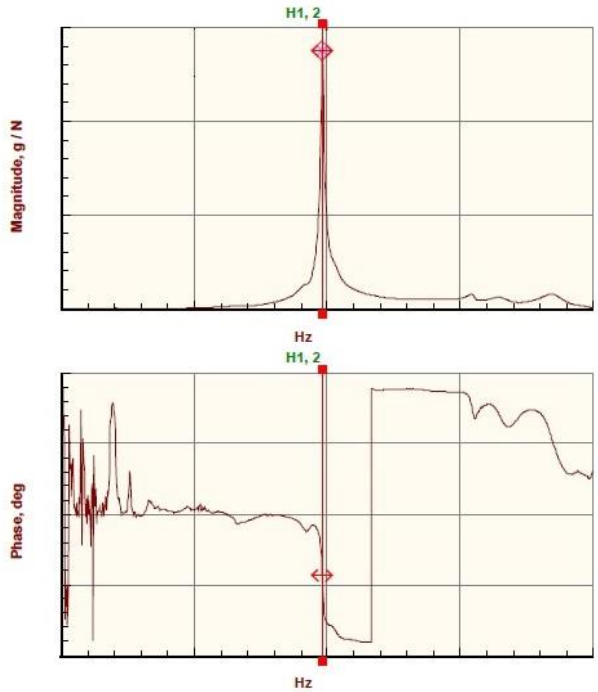

Figure 19: Tail rotor drive shaft model validation for the lowest frequent bending eigenmodes (based on ground test data / hammer impact test)

In-flight acceleration measurements at the tail rotor drive shaft bearings were used as an indicator for the magnitude of the shaft's bending motion (at 1/rev drive shaft speed frequency) which results from the unbalance of the shaft and a possible dynamic amplification on top. Like predicted by the validated simulation model, flight test data confirmed the good frequency placement, as a variation of rotor speed did not show any sign of resonance frequency close to the operative range (see Figure 20).

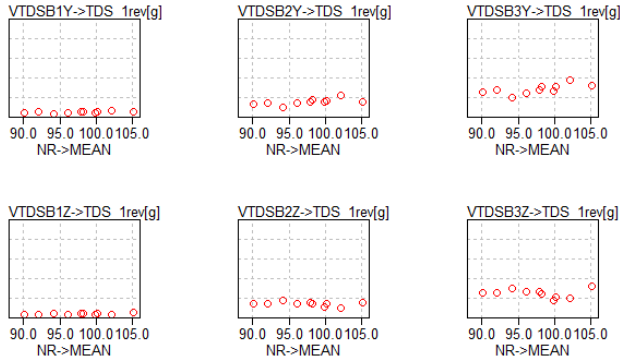

Figure 20: Accelerations at tail rotor drive shaft bearings vs. main rotor speed (flight test data)

Despite the imposed challenge of increased drive train speed range together with a reduced nominal speed, an excellent dynamic layout has been achieved for the tail rotor drive shaft based on the simulative approach. This result highlights the capabilities of a simulation based design approach.

4. GROUND AND AIR RESONANCE

Ground resonance stability calculations were performed with a FE-model of the airframe on ground coupled to the multi-body main rotor model.

The model components were validated by whirl tower test results of the main rotor and a shake test of the airframe on ground. Additionally the lead-lag damper properties were adjusted according to component test results. These tests were performed on the dampers actually integrated in the BLUECOPTER DEMONSTRATOR's main rotor.

Air resonance stability was investigated in a similar manner, using in that case the inertia characteristics of the airframe and free flight degrees of freedom instead of the grounded elastic FE-model.

The results of the calculations with the validated sub-models were used to pave the way for the permit to fly for the BLUECOPTER DEMONSTRATOR. Due to the large main rotor blade inertia compared to the airframe, the BLUECOPTER configuration was assessed to show potential aeromechanic challenges and it was decided to start flight testing with a restricted rotor speed envelope. Based on extensive flight testing and a good agreement of the analysis with the test results, the initially introduced rotor speed restrictions could be lifted.

4.1. Ground Resonance

Flight test clearance was achieved based on a comprehensive simulation study featuring a coupled rotor-airframe model. Thereby, the elastic properties of the airframe were derived by FE modelling (see Figure 21) and integrated into the multi body rotor model (CAMRAD II model; see section 2) in form of linear normal modes.

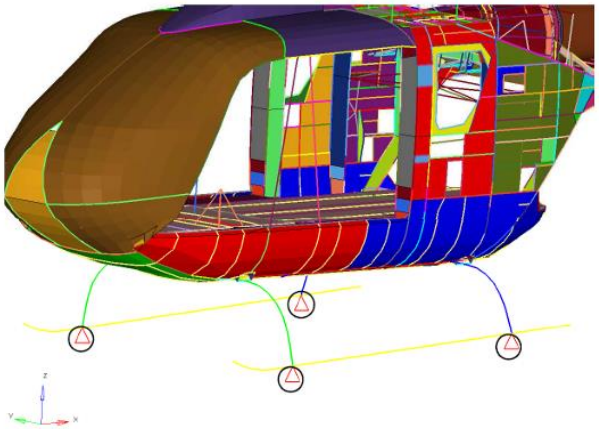

Figure 21: Elastic airframe model (FE) for ground resonance investigations

Through a shaker test campaign of the complete helicopter, eigenmodes for the helicopter on ground were identified for different ground surfaces (concrete, grass) and different weight configurations. This data was used for validating the airframe model, similar to the approach for the main rotor where whirl tower test results allowed validating the rotor model. Parallel to the fully elastic airframe model, a reduced model setup, featuring an elastic landing gear and a rigid fuselage, was investigated.

The simulation study covered a variation of the following parameters:

- Helicopter weight and balance (low/mid/high weight; C.G. forward/mid/aft)
- Ground surface condition (soft/stiff)
- Lead-lag damper operating condition (low/mid/high amplitude/temperature)

Special focus was put on the sensitivity of M/R lead-lag damper properties regarding temperature and displacement amplitude which both affect stiffness

and energy absorption (damping) characteristics. Adequate stability margins were predicted for all investigated conditions.

Ground testing involved various H/C weight and balance configurations as well as testing on different ground surfaces. Good agreement with the simulation model was found (see Figure 22), confirming the capability of the simulative approach. No ground resonance condition occurred during the test, shown in the figure. The calculated damping is conservative.

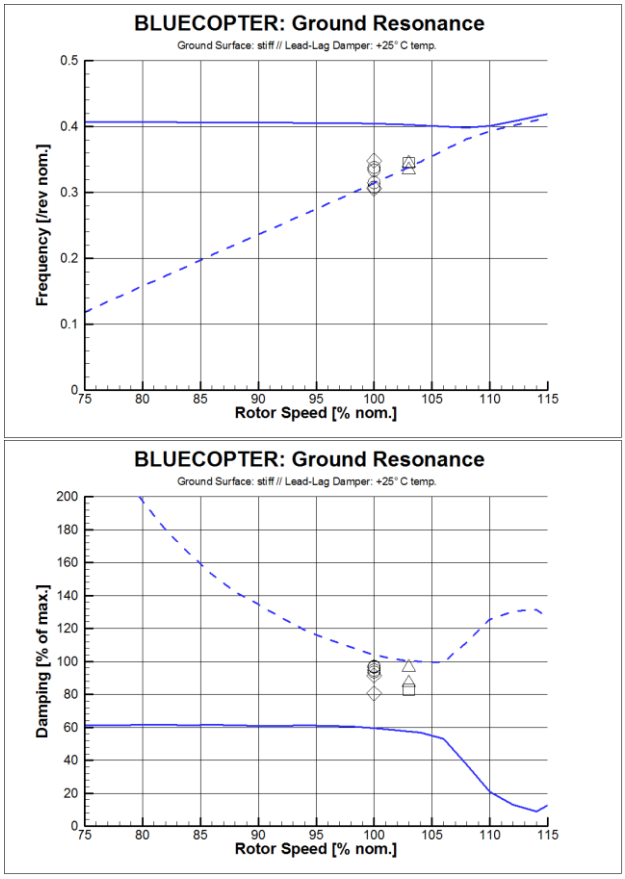

Figure 22: Validation of the ground resonance simulation model by ground test data

4.2. Air Resonance

Similar to the simulation approach for ground resonance, a coupled rotor-airframe model, based on the validated CAMRAD II rotor model, was used. However, here the airframe was modelled as a rigid element, featuring inertia properties according to the helicopter's weight and balance configuration. This approach is valid as the elastic deformation of the fuselage during air resonance conditions is of minor influence due to the missing boundary conditions (ground contact).

Besides analysing H/C weight and balance configurations and studying the operative range of lead-lag damper properties, different operating conditions have been investigated:

- Ambient conditions
  (altitude, temperature)
- Flight manoeuvres
  (level flight, climb/descent, autorotation)

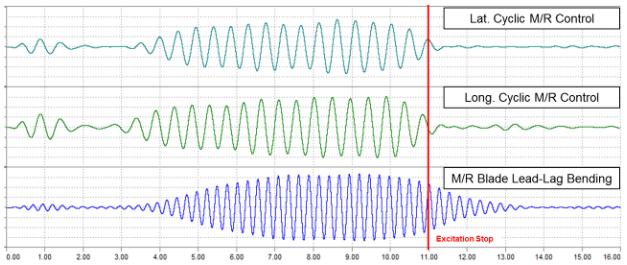

Figure 23: In-flight measurement of air resonance stability margins (pilot stick whirl excitation)

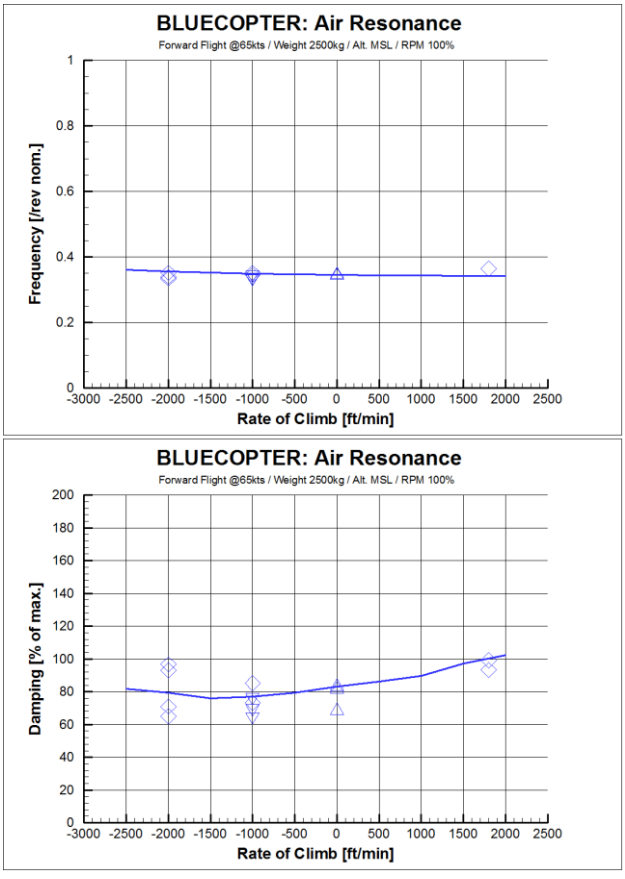

Figure 24: Validation of the air resonance simulation model by flight test data

Initial results indicated adequate stability margins for nearly the whole flight envelope. However, as the

lowest margins were predicted for high rotor speeds, an NR limit was introduced at the start of the flight test campaign.

As for ground resonance testing, frequency and damping identification of the lowest coupled rotor-airframe mode has been performed by pilot cyclic stick whirl excitation and analysis of the decay curves (see example in Figure 23).

Based on the robust stability margins measured in flight, conservatism in the modeling approach could be identified within the model validation loop.

The updated model shows good agreement with flight test results (see Figure 24) and was used for recalculating the most critical scenarios which finally allowed lifting the initially introduced NR limitation.

5. CONCLUSION AND OUTLOOK

The BLUECOPTER DEMONSTRATOR has been developed to demonstrate the ability to design an eco-friendly helicopter. Especially the noise reduction measures were a challenge for dynamics.

The low tip speed required blades with large inertia to fulfill lock number requirements and to reduce the first lead-lag frequency to reasonable values for lead-lag loads. The low tip speed also leads to a high advance ratio compared to standard designs. This has a potential negative impact on blade loading in fast forward flight condition.

The large rotor speed range made the blade tuning quite difficult. Especially the second lead-lag mode suffered from the large speed range.

The innovative planform also was a challenge for blade tuning as the swept forward area required a special tuning mass to ensure flutter stability. This mass was bound to a certain radius position. Additionally no tuning masses could be used near the blade tip, as this would also have decreased flutter stability margins as the blade tip is strongly swept backwards.

Most parts of the EC135 drivetrain were reused for the BLUECOPTER DEMONSTRATOR. The Fenestron® driveshaft had to be modified due to the elongated tailboom of the helicopter. Additionally the Fenestron® was equipped with BlueEdge™ style blades to reduce noise emission after gaining some experience with the standard EC135 Fenestron®. Sufficient safety margins regarding torsional stability and critical speeds were shown, even for the significantly slower rotational speed with large speed variation.

Due to the large rotor blade inertia compared to the “small” airframe a potential risk for air resonance was assumed, which lead to a preliminary flight envelope restriction. The first flight tests showed sufficient margins and validated the models. So the flight envelope restriction could be lifted.

The BLUECOPTER DEMONSTRATOR’s design was enabled from a dynamics point of view despite strong constraints from requirements for eco-friendly design. Compromises were mainly made within the topic of blade frequency placement in relation with the low tip speed and the rotor speed range.

For future eco-friendly helicopter designs, which aim more at serial applications more refined trade-offs between dynamics and eco-friendliness requirements will be targeted when selecting planform, blade tip speed and rotor speed range. For serial application in the near future the extremely low tip speed and the very large rotor speed range, which were demonstrated with the BLUECOPTER DEMONSTRATOR, are probably not used to its full extend. This will ease the dynamic layout of blades, drive train and overall helicopter.

On the other hand, it could be shown that by a convergent development and test Logic based on dynamics tools application and model validation the challenges posed by multidisciplinary optimization with the weighting on eco-friendly disciplines can be adequately treated.

6. REFERENCES

[1] Rammer, R., Priems, M., Konstanzer, K., “Modification of a Four Bladed Main Rotor – Impact on Dynamics and Vibrations” 39th European Rotorcraft Forum, Moscow, Russia, September 2013.

[2] Schneider, S., Heger, R., “BluecopterTM Demonstrator: The State-of-the-Art in Low Noise Design”, 43rd European Rotorcraft Forum, Lille, France, September 2016.

[3] Bebesel, M., D’Alascio, A., Schneider, S., Guenther, S., Vogel, F., Wehle, C., Schimke, D., “BLUECOPTER DEMONSTRATOR – an Approach to Eco-Efficient Helicopter Design”, 41st European Rotorcraft Forum, Munich, Germany, September 2015.

[4] Rauch, P., Gervais, M., Cranga, P., Baud, A., Hirsch, J.F., Walter, A., Beaumier, P., “BlueEdge™: The design, development and testing of a new blade concept“, AHS 67th Annual Forum, Virginia Beach, VA, May 2011.

[5] van der Wall, B., Kessler, C., Delrieux, Y., Beaumier, P., Gervais, M., Hirsch, J.F., Pengel, K., Crozie, P., "From ERATO Basic Research to the Blue Edge^{TM} Rotor Blade", AHS 72nd Annual Forum, West Palm Beach, Florida, May 2016.

[6] Kneisch, T., Krauss, R., D'Alascio, A., Schimke, D., "Optimised Rotor Head Design for an Economic Helicopter", 37th European Rotorcraft Forum, Vergiate and Gallarate, Italy, September 2011.

[7] Schneider S., Mores S., Edelmann, M., D'Alascio, A., Schimke, D., "Drag Analysis for an Economic Helicopter", 37th European Rotorcraft Forum, Vergiate and Gallarate, Italy, September 2011.

[8] Gubernatis, S., Weiland, F., Stockhausen, A., Hellmich, J., "Integrating Textile Preform Process Chains – from 2D Flat Product to 3D Preform" SAMPE 2013 Long Beach, Long Beach, USA, May 2013.

[9] Springl, F., Welz, P., Zaremba, S., Weimer, C., Drechsler, K., "Multi-component LCM Processing for Aeronautical Structural Applications – the Influence of Deflection in Metering and Homogenization", Flow Processes in Composite Materials FPCM – 11, Auckland, New Zealand, July 2012.

[10] Johnson, W., "Technology Drivers in the Development of CAMRAD II", AHS Specialist's Conference on Aeromechanics, San Francisco, CA, January 1994.

[11] Cranga, P., Krysinski, T., Strehlow, H., "GAHEL – a General Code for Helicopter Dynamics" AHS 60th Annual Forum, Baltimore, MD, June 2004.